2023

Impacts of hydrodynamic regimes on the resuspension of particulate matter within a seagrass restoration site: Jennycliff Bay, Plymouth Sound, UK

Bevington, L.M.

Bevington, L.M. (2023) 'Impacts of hydrodynamic regimes on the resuspension of particulate matter within a seagrass restoration site: Jennycliff Bay, Plymouth Sound, UK', The Plymouth Student Scientist, 16(1), pp. 1-24.
https://pearl.plymouth.ac.uk/handle/10026.1/21080

The Plymouth Student Scientist
University of Plymouth

*The Plymouth Student Scientist, 2023, **16**, (1), 1-24*

Impacts of hydrodynamic regimes on the resuspension of particulate matter within a seagrass restoration site: Jennycliff Bay, Plymouth Sound, UK

Laura M. Bevington

Project Advisor: Dr Phil Hosegood, School of Biological and Marine Sciences, University of Plymouth, Drake Circus, Plymouth, PL4 8AA

Abstract

Seagrass habitats are ecosystem engineers, providing a multitude of valuable ecosystem services that benefit the environment and human populations. Seagrass meadows are declining at an enhanced rate; therefore, in recent years restoration efforts have increased. However, many projects have had limited rates of success. Site suitability assessments are conducted ahead of plantation efforts; however, some regimes are seldom considered despite them providing important insights into a site's environmental conditions. For example, light availability to the benthos is a key component of restoration success and this is affected by hydrodynamic processes impacting the local resuspension regime of suspended particulate matter (SPM), and therefore water clarity.

This study assesses the local SPM resuspension regime within the active seagrass restoration site known as Jennycliff Bay, Plymouth Sound, UK. Multiple surveys were conducted to assess the temporal variation in SPM concentrations. An oceanographic mooring provided a 7-week time series of current velocity and echo intensity (EI) measurements. Water samples' SPM concentrations were determined using optical backscatter (OBS) data. OBS measurements were converted into mg/l values and used to validate the use of EI as a proxy measurement of SPM concentrations.

A background resuspension regime was observed within Jennycliff Bay with SPM concentrations influenced by tidal cycles. Maximum SPM concentrations were observed ~2m above the seabed during an ebbing tidal phase. Peak in-situ EI measurements confirmed the occurrence of SPM re-settlement. Current velocities measured throughout the study were relatively modest, with a maximum current velocity of 0.28m/s observed throughout a flooding tide; an in-situ bed shear stress (BSS) values measured 0.15N/m2, only 0.01N/m2 below the maximum observed value, throughout the 7-week dataset. A clear correlation between current velocity, BSS and EI confirmed the relationship between hydrodynamic processes and SPM concentration. Furthermore, these results identified the influence of storm forcing, amplifying all the considered variables.

This study can not only be used to advise seagrass restoration efforts within Jennycliff Bay, but also highlights the importance of assessing hydrodynamic regimes and local SPM resuspension within a proposed restoration site; therefore, the study can be carried forward and used as guidance for future research.

Keywords: suspended particulate matter; echo intensity; bed shear stress; sediment resuspension; seagrass restoration.

Introduction

Seagrass

Seagrasses are marine angiosperms (Hemminga and Duarte, 2000); they are often referred to as ecosystem engineers, predominantly found in shallow coastal regions (Adams *et al.,* 2016; van der Heide *et al*., 2011; Waycott *et al.,* 2009). Seagrass meadows provide a multitude of ecosystem services such as carbon sequestration, nutrient cycling, and sediment stabilisation (Hyman *et al.,* 2019; Apostoloumi *et al.,* 2021). Nevertheless, habitats have declined at a rate of ~7% per year since the 1990's, as human activity in coastal regions has increased with global development (Waycott *et al*., 2009; van Katwijk *et al*., 2016).

Studies have identified that healthy meadows are able to reduce significant wave height by ~20-50%, alleviating wave impact across adjacent shorelines (Paul and Amos, 2011; Infantes *et al*., 2012; Reidenbach and Thomas, 2018). Wave attenuation decreases BSS, and thus SPM throughout the water column (Carr *et al.,* 2012). Additionally, the complex root systems of seagrass meadows further encourage sediment stabilisation. These ecosystem services encourage a positive feedback loop; increasing light propagation through the water column, further facilitating seagrass growth (van der Heide *et al*., 2011; Maxwell *et al*., 2017; Walter *et al*., 2020). Walter *et al*. (2020) identified the loss of seagrass meadows would likely alter local hydrodynamics, leading to increased rates of coastal erosion, suggesting seagrass meadows provide a natural solution to coastal defence requirements, highlighting the importance of habitat preservation.

Storm surges have been identified as a significant threat to seagrass habitats (Orth *et al*., 2006; Suykerbuyk *et al.,* 2016; van Katwijk *et al*., 2016); increased current velocities, a consequence of storm activity, prematurely removes plant foliage, reducing rates of photosynthesis (Hemminga and Duarte, 2000). Furthermore, storm activity increases SPM resuspension, destabilising the seabed, compromising seagrass root establishment (van Katwijk *et al*., 2016).

Due to the rate of habitat loss, and the increased awareness of meadows' ecosystem roles, seagrass restoration development projects have increased in recent years (Orth *et al*., 2006; Unsworth *et al*., 2018). However, success rates vary throughout restoration efforts (Zhou *et al*., 2014; Suykerbuyk *et al.,* 2016; Xu *et al*., 2020). Seagrass seedlings are susceptible to burial and physical damage; therefore, projects exclusively using seedling have limited success (van Katwijk *et al*., 2016). Greater restoration success is observed throughout projects that adopt the use of anchoring systems or rigid frameworks (Tan *et al*., 2020; Carus *et al*., 2021). The use of artificial seagrass generation (ASG) methods stabilises local sediments, promote positive feedback loops, and buffer unsuitable hydrodynamic regimes, ultimately promoting restoration success (Carus *et al*., 2021).

Suspended Particulate Matter

A key requirement for seagrass survival is light availability, which can be impacted by suspended particulate matter (SPM) concentrations within the water column (Ralph *et al*., 2007; Collier *et al.,* 2012; Adams *et al.,* 2016; van Katwijk *et al*., 2016). Adams *et al.* (2016) identified that intact seagrass meadows promoted a positive feedback loop, referred to as the seagrass-sediment-light (SSL) feedback. The SSL promotes sediment deposition, water clarity and light availability at the benthos, supporting photosynthesis and meadow survival (Gacia and Duarte, 2001; Adams *et al.,* 2016). However, this positive feedback can lead to environment bistability (Adams *et al.,* 2016; Carus *et al.,* 2021). As seagrass biomass is lost, the sediment becomes susceptible to resuspension, increasing

SPM concentrations, thus reducing light availability, and inhibiting seagrass meadow regeneration. The SSL feedback has been identified as a major barrier to the successful conservation and restoration of the temperate species *Zostera marina* (van der Heide *et al*., 2011). Carus *et al*. (2021) highlights the significance of a bistable environment, explaining that once a system has shifted due to a disturbance, such as vegetation loss, the recovery is challenging. Van der Heide *et al.* (2011) identified that the SSL feedback was the dominant mechanism controlling the success of seagrass restoration in exposed areas. The importance of understanding the bistability and SPM regime within a potential restoration location is clear, and in doing so, will enable the development of appropriate restoration methods.

Studies have highlighted the difficulties determining species specific SPM thresholds (Lee *et al.,* 2007; Collier *et al.,* 2012). Due to this lack of knowledge specific to seagrass meadows, assumptions are generally made using data acquired for species in other ecosystems, such as coral reefs (Collier *et al.,* 2012). Sofonia and Unsworth (2010) identified a significant correlation between SPM, light availability, and seagrass biomass, suggesting SPM data could be used as an indicator for seagrass meadow survival potential; however, this relationship was met with caution. Nevertheless, the relationship between light availability and meadow biomass has been widely studied, with findings identifying that extended light availability sustains seagrass growth (Ralph *et al*., 2007; Sofonia and Unsworth, 2010; van der Heide *et al*., 2011; Collier *et al.,* 2012).

Furthermore, Cabaço *et al.* (2008) identified an increased risk of seagrass burial from re-settling SPM, as previously enhanced current velocities subsided. However, burial thresholds vary between seagrass species and is significantly size-dependent. Importantly, smaller meadows are more susceptible to burial; therefore, a site's sediment resuspension regime must be considered when conducting restoration site assessments (Cabaço *et al*., 2008).

Bed shear stress (BSS)

The impact of hydrodynamic processes on BSS

Carr *et al.* (2012) identified a relationship between increased BSS and SPM concentrations. Friction at the seabed is increased as hydrodynamic processes, such as current flows, are amplified by storm events, increasing BSS and causing the resuspension of particulate matter (Carlin *et al.,* 2016; Alekseenko and Roux, 2020). Current velocities around coastal regions have two components: tidal and residual, therefore both must be considered when assessing current velocities, BSS, and consequently SPM concentrations. Tidal current velocity regimes are influenced by the tidal cycle and are therefore predictable. Residual currents are a product of external forcing, influenced by wind speed and waves (Lawson *et al.*, 2007).

Calculating BSS

Multiple studies have assessed site specific BSS and its relationship with SPM concentrations (Tattersall *et al.,* 2001; Carr *et al.,* 2012; Uncles *et al*., 2015; Carlin *et al.,* 2016; Alekseenko and Roux, 2020). Studies often determine a critical erosion threshold/ critical shear stress value, providing a site-specific threshold for sediment resuspension (Carr *et al.*, 2012; Carlin *et al.,* 2016; Alekseenko and Roux, 2020). Two studies within Plymouth Sound assessed the variation in BSS and SPM throughout tidal cycles, whilst considering variations in current velocities and significant wave height (H_s) (Tattersall *et al*., 2001; Uncles *et al.,* 2015). Tattersall *et al*. (2001) identified that BSS increased as tidal ranges transitioned from neap to spring, resulting in increased current velocities. Uncles *et al*. (2015) identified the average BSS within Plymouth Sound, related to the M_2 tidal

hormonic, which ranged between 0 to 0.65N/m^2, with greater stress values observed in areas with greater grain sizes. Both studies identified the average SPM concentrations within Plymouth sound ranged from <2mg/l to 5mg/l (Tattersall *et al.*, 2001; Uncles *et al.,* 2015). A later study conducted by Carlin *et al*. (2016) presented further evidence that a combined effect of residual current velocities and BSS, impacted SPM concentrations, confirming the importance of incorporating hydrodynamic processes into restoration site suitability assessments.

Using echo intensity (EI) as a proxy measurement of SPM

Optical and acoustic techniques have been used to assess site specific SPM concentrations (Hill *et al.,* 2002; Chanson *et al.,* 2007; Spearman *et al.,* 2020; Manik *et al.,* 2021). Generally, SPM concentrations are obtained using OBS data and in-situ water sample analysis. However, some studies have favoured the use of models to predict temporal variation in SPM (Hill *et al*., 2002; Chanson *et al*., 2007). Hill *et al*. (2002) assessed sediment resuspension rates using an acoustic doppler current profiler (ADCP) together with modelled SPM concentrations. The study identified a relationship between ADCP EI and SPM concentrations, determining the presence of a background SPM resuspension regime, coinciding with the semi-diurnal tidal cycle (Hill *et al.,* 2002). The main limitation identified within Hill *et al's.* (2002) study was that acoustic techniques did not reliably distinguish grain size classification. Therefore, it is suggested to assume a uniform grain size when assessing the variation in EI, relative to fluctuations in SPM concentrations. A later study conducted by Chanson *et al*. (2007) also used EI as a surrogate measurement of SPM, further validating the technique.

Spearman *et al.* (2020) used OBS and ADCP data to identify the behaviour of deep-sea sediment plumes. OBS data was used to validate increases in EI signals, confirming a relationship between increasing SPM and increased EI. Once the relationship was verified, Spearman *et al.* (2020) were able to determine the extent of a sediment plume by solely analysing the EI signal. Recently, Manik *et al.* (2021) utilised an ADCP to quantify SPM; the study found a strong correlation between increased EI and SPM whilst highlighting the impact of enhanced current strengths on SPM concentrations.

Previous studies have established the relationship between light penetration and SPM, therefore, the impact of local hydrodynamic regimes on SPM has the potential to affect the suitability of seagrass restoration sites. The purpose of this study is to assess the SPM resuspension regime within the seagrass restoration site at Jennycliff Bay, Plymouth Sound, UK. Data will be used to quantify the temporal variability in tidal and residual current velocities, BSS, and consequently SPM concentrations throughout a 7-week period. The results will provide an insight into the hydrodynamic regimes within the area, contributing to the assessment of the site's suitability for seagrass restoration. The findings will further advise restoration efforts on appropriate plantation timings and methods, therefore promoting restoration success.

Methodology

Study area

Jennycliff bay is a shallow sandy bay located within the eastern area of Plymouth Sound. The chosen study area is located outside of the designated anchoring restriction zone of Jennycliff Bay, adjacent to the southwest tip of the active seagrass restoration site (figure 1). Throughout August and September 2021, several surveys were conducted within the study site (figure 1), aiming to acquire current velocity, BSS, EI, and SPM concentration measurements throughout varying tidal phases and meteorological conditions (table 1).

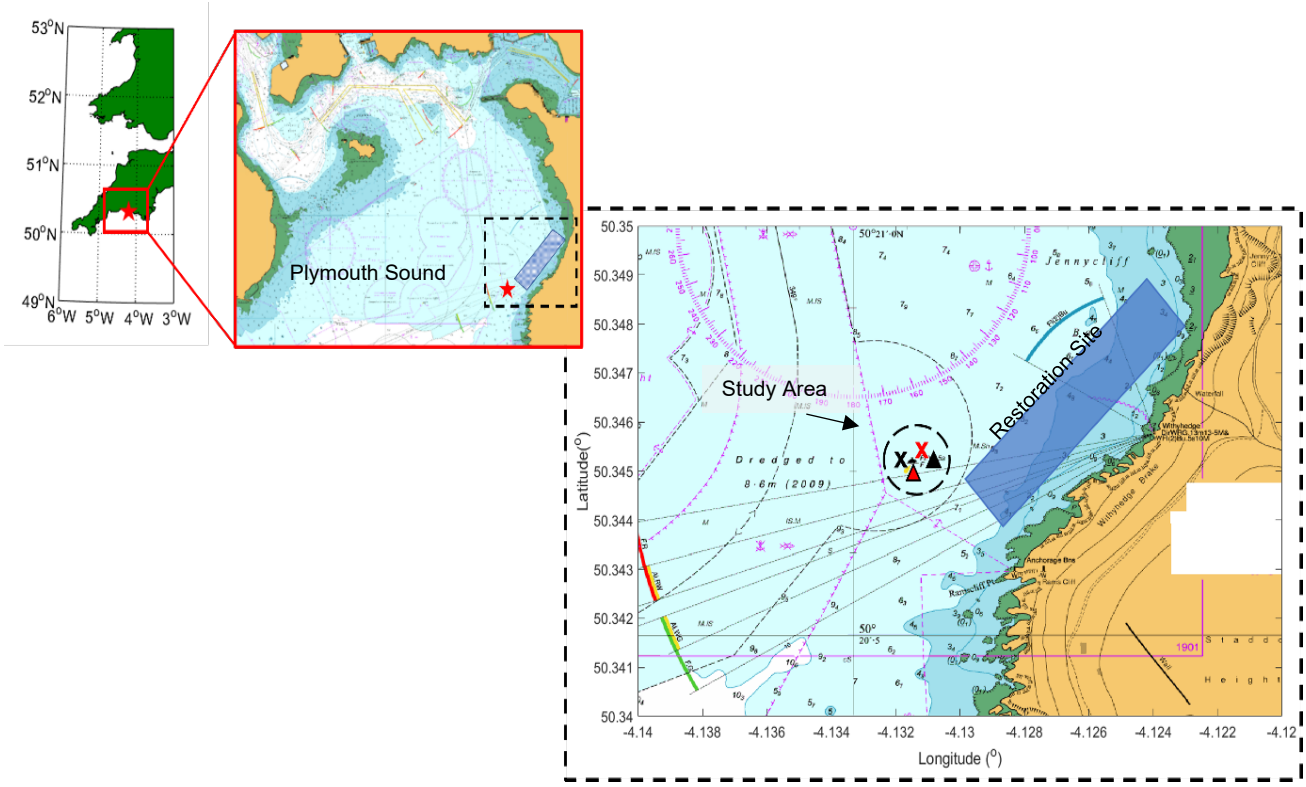

Figure 1: The survey site location of Jennycliff Bay, Plymouth Sound, UK. Red star: location of the oceanographic mooring, 50°20.695'N 004°07.883'W (Degrees Minutes and Seconds: DMS). Blue box: designated seagrass restoration area within Jennycliff Bay. Black circle: 50m radius surrounding the oceanographic mooring. Vertical OBS profile positions: P1 – P8 (black cross); P9 – P17 (red cross); Black triangle: S2; Red triangle: S1 and S3. Latitude and longitude coordinates shown on the image are in decimal degrees: DD (image source: Digimap Edina).

Table 1: A summary of the survey conditions including Low Water (LW), High Water (HW), Tidal Range (TR), Tidal Phase (TP) and the sea state. LW and HW times predicted for Devonport, Plymouth, UK**.**

Date	LW	HW	TR	TP	Wind	Sea state
01/09/2021	19:49 @ 2.54m	13:12 @ 4.20m	1.66m	Neap	NE/E 10-14kt	Calm/slight
07/09/2021	06:55 @ 5.22m	13:04 @ 0.93m	4.29m	Spring	E 7-13kt	Calm/slight
29/09/2021	16:59 @ 2.45m	11:16 @ 4.40m	2.05m	Neap	NW 12-22kt	Slight/choppy

Assessment of the temporal variation in SPM

To assess the temporal variation in SPM concentrations, throughout contrasting tides, vertical profiles were collected. A SBE 19 Plus Seacat CTD V2, equipped with an optical backscatter sensor (OBS), was deployed from *RV Dolphin* on the 01 September 2021 (figure 1). A total of 17 vertical water column profiles (P1-P17) were collected (table 2). One vertical profile was collected every 10minutes for 1.25hours during the flood and ~2 hours during the ebb. Voltage measurements obtained in 0-1m depth were discarded due to air contamination; values captured between 1-2m depth, within each vertical profile, were averaged, removing any dataset noise captured during the sensor calibration.

Table 2: A summary of the raw voltage data collection parameters, 01 September 2021 including the time stamp of each survey. Latitude and longitude provided in DMS.

Date	Profile	Max Depth	Latitude (N)	Longitude (W)	Tidal Phase	Time
01/09 (AM)	P1-P8	12.3 - 12.8m	50˚20.693	004˚07.886	Flood (Neap)	10:15-11:30
01/09 (PM)	P9-P17	12.5 - 14.2m	50˚20.695	004˚07.915	Ebb (Neap)	13:59-15:49

Water sample collection

Water samples were collected at three station locations (S1-S3) to resolve vertical variations in SPM concentrations adjacent to the seagrass restoration site (figure 1). Water samples were collected using a CTD Rosette sampler equipped with 6 Niskin bottles, an SBE 19 Plus Seacat CTD V2 and an OBS. The calibration for both the CTD and OBS instruments was consistent throughout all surveys. The instrumentation was deployed from *RV Falcon Spirit* on the 7th and 29th of September 2021. Bottom, mid, and surface water samples were obtained at each station along with in-situ volt measurements (table 3).

Table 3: A summary of the CTD Rosette deployment conditions, locations (DMS), and the data/sediment collection parameters, 07 and 29 September 2021.

Station	Surface	Mid	Bottom	Latitude (N)	Longitude (W)	Tidal Phase
S1 – 07/09	1.9m	5.6m	10.6m	50˚20.697	004˚07.885	Ebb – Spring
S2 – 07/09	3.7m	6.1m	8.3m	50˚20.701	004˚07.875	Ebb – Spring
S3 – 29/09	1.4m	5.6m	10.7m	50˚20.697	004˚07.885	Ebb – Neap

Water sample filtration and SPM calculations

A filtration method was utilised to determine the total concentration of SPM within the acquired water samples at S1-S3, following the method of Strickland and Parsons (1972). A given volume of seawater, *V*, was filtered through pre-dried and weighed Camlab Garde 263(F) 0.7micron (µm) glass microfiber filters, using a 25mm filtration apparatus. A vacuum of 300-400mmHg was applied throughout the filtration process. Pre-dried filters were weighed using a Sartorius analytical five-figure balance, this weight was defined as f_a. For filters used as blanks, this number became *b1*. Once filtered, sediment samples were dried at 60 ˚C for 24 hours, and then transferred to a desiccator for three days. Post drying, the filters were re-weighed (3 times each) providing average final weights (f_b), and for the blanks, *b2*. Two blank filters were used throughout the filtration process, providing a mean blank correction value (*b*) of 6.16 x 10^{-5} mg/l. SPM values were obtained using the

equation *((f_b + b) - f_a)/V*. The standard deviation (SD) of SPM values was 7.99 x 10^{-4}, obtained from three triplicate filtrations. This processing resulted in an output of 8 SPM concentration datapoints.

Organic / inorganic particulate fractions
To determine the percentage composition of organic/ inorganic particulates within each sample, samples were placed into a *Muffle Furnace* and ashed. Samples were then re weighed, providing a third weight (*f_c*) of purely inorganic particulate matter. The inorganic fraction *(*SPMin*)* of each sample was resolved using the equation, *SPMin = ((f_c + bi) – f_a)/V,* where *bi* is defined as the mean weight of two ashed blank filters (*b1* and *b2*). The organic component (SPMo) was obtained using the equation, *SPMo = SPM – SPMin. SPMo* and *SPMin* values were later converted into percent values.

Calibration equation: converting voltage values to SMP concentrations
A calibration equation was created (equation 1) using 5 randomly selected datapoints (N = 5) from the S1-S3, 8-datapoint SPM dataset. The remaining 3 SPM datapoints were withheld for an independent calculation of root mean square error (RMSE). Statistical tests were applied using a correlation coefficient (alpha = 0.01 (99%)) together with a p-value of 0.0024. As $p < 0.01$, the correlation was deemed significant with a 99% confidence in the linear regression r^2 (0.9421) and y (17.688) value.

$$SPM = 17.688 \times Voltage \ (r^2 = 0.9421, p < 0.01, N = 5, RMSE = 0.44 \ mg/l) \quad (1)$$

Equation (1) was then applied to the downcast OBS volt values measured throughout the 01/09, converting raw voltage data into SPM concentration values.

Oceanographic mooring
To assess the temporal variation in EI and current velocities within Jennycliff Bay, a broadband WorkHorse monitor, RDI 600kHz ADCP, housed within an MSI bedframe, was deployed at the seabed (figure 1). The mooring was deployed for a duration of 7 weeks, between the 11 August and 29 September 2021. The ADCP was mounted 0.5m above the seabed (beams up), sampling at 2Hz, with a blanking distance of 1m; the first bin was collected at 1.6m. EI and current velocities were measured every 10 seconds, with 9 pings per ensemble. Data was internally averaged into 0.5m bin cells. All current data was cleaned and averaged using a 9-point moving average within MATLAB.

Inferring local resuspension (SPM) from ADCP EI
EI data was used as a proxy measurement to assess the temporal variation in SPM. To remove the attenuation of echo amplitude with range, the time-mean amplitude for each depth was removed. Demeaned EI data was then smoothed. Datapoints collected on the 01/09 were smoothed using a 10-minute moving average. As the dataset of interest was <24hours in length, a 10-minute moving average enabled smoothing without compromising resolution. This smoothing aligned EI data with in-situ SPM vertical profiles, allowing direct comparisons of measurements. The aim of this process was to validate the use of EI as a proxy indication of SPM concentration throughout the 7-week timeseries. A 1-hour moving average was applied when processing the entire 7-week dataset.

Influence of tidal regime on observed current velocities
Local tidal characteristics and regimes were assessed using TPX07 (ES2008) and T_Tide models within MATLAB; TPX07 provided a tidal height (z) prediction throughout the 7-week period, T_Tide analysed the local tidal harmonics. T_Tide also extracted the tidal

current velocity component within the dataset, enabling the identification of residual current velocities. Previous studies acknowledged the validity in using T_Tide when assessing tidal harmonics (Pawlowicz *et al*., 2002; Uncles *et al*., 2015). These model outputs provided a tidal characteristic prediction however do not account for forcing factors influencing a tidal flow therefore the model outputs were used as reference points when resolving the 7-weeks of current measurements from the ADCP.

The temporal variation in current velocity was measured to assess the impact of tidal regimes and enhanced flows on SPM concentrations. Current data was handled similarly to EI data; for data analysis on the 01/09, both V and U velocity data were smoothed using a 10-minute moving average. When processing the entire 7-week dataset, U and V velocity data were smoothed using a 1-hour moving average. Data were handled in the same way for both EI and current velocity, enabling direct comparison of temporal variations.

Determining BSS

To calculate the BSS, τ_b, two equations were used. Firstly, the frictional shear velocity, U_*, was calculated using the Von Karman – Prandtl equation (equation 2). The dominant current velocity component within the survey area was deemed to be V (north/south), therefore, measured V velocities were solely used within this equation. The bed roughness length (z_o) was assumed to be 0.0003m following the findings of Uncles *et al*. (2015) and Fitzpatrick (1991). The selected z_o value is appropriate for a poorly sorted (sandy) bed type classification (Fitzpatrick, 1991; Soulsby, 1997; Uncles *et al*., 2015). The height above bed (HAB), *z*, also remained constant at 2m, V current velocities were not measured below this depth. The *z* value of 2m remained constant as this study focused on measurements close to the seabed.

$$\frac{V}{U_*} = \frac{1}{k} * ln\left(\frac{z}{z_o}\right)$$
$$\frac{V}{U_*} = \frac{1}{0.4} * ln\left(\frac{2}{0.0003}\right)$$
$$U_* = \frac{V}{22.012} \quad (2)$$

V is defined as the current speed (m/s), U_* is the frictional shear velocity (m/s), *k* is the von Karman's constant (0.4), *ln* is the natural logarithm of (z/z_o), *z* is the height above bed (2m) and z_o is the bed roughness length of 0.0003m (Dyer, 1997, p.48).
The calculated U_* value was used to calculate BSS, τ_b, for the 7-week timeseries using V current velocity data (equation 3). A water density (ρ) value of 1025.5kg/m^3 was selected as a constant, determined using in-situ CTD measurements.

$$\tau_b = \rho U_*^2 \quad (3)$$

BSS is defined as τ_b, ρ is water density (1025.5kg/m^3) and U_*^2 is the frictional shear velocity squared (Dyer, 1997, p.50).

Storm forcing of wind and waves

MetOcean data was downloaded from the Plymouth Coastal Observatory (PCO) quality controlled (QC) historical database (PCO, 2022). Wave data measurements were

collected via Looe Wave Buoy, located 50° 30.32′ N and 004° 24.64′ W (DDM). Meteorological data was measured from a met station located 50° 20.70′ N and 004° 27.17′ W (DDM). Wind and wave data were downloaded for August and September to assess the relationship between storm events, enhanced wind speeds and H_s, and hydrodynamic regimes. Wind and wave direction data were also obtained; all data was processed within MATLAB.

Results

Influence of tidal regimes on current velocities (tidal and total)

Observations of the T_Tide model output highlight that within the study area the M_2 tidal harmonic is dominant, with a prevalent V current flow (figure 2A). TPX07 predict that the maximum spring, and minimum neap, tidal ranges experienced throughout the survey period were 5.24m and 1.1m respectively (figure 2B).

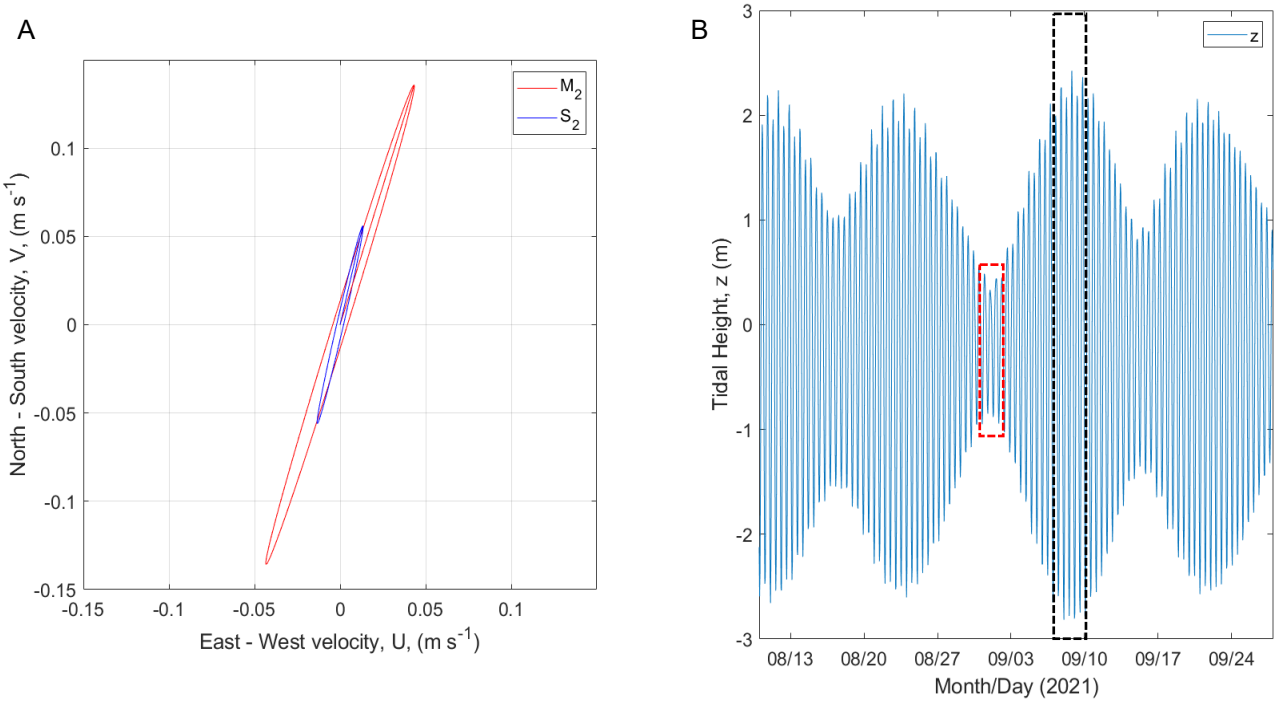

Figure 2: A) Tidal ellipse output from T_Tide. M_2 (red) and S_2 (blue) tidal harmonics identify the dominance of each tidal frequency within the ADCP data. **B)** Tidal height prediction output from TPX07 ES2008 for the 7-week deployment length (11/08/21 – 29/09/21). Black box: maximum spring tidal range (07/09/21). Red box: minimum neap tidal range (01/09/21).

A background current velocity regime within Jennycliff Bay can be observed within the measured ADCP data (figure 3). It is also noted that tidal current velocities are influenced by the tidal cycle regime, with flow speeds oscillating with the tidal phase (figure 3). The point at which maximum tidal current velocities were observed throughout the tidal cycles varied with spring/neap tides (figure 3). Throughout the timeseries, it was observed that the tides are asymmetric, the flooding tide lasts for ~4 hours; whereas it takes ~8hours for the tide to ebb (figure 3).

A maximum tidal current velocity of 0.23m/s was measured in the northward (V) direction, at HAB:2m, on the 07/09 when the maximum spring range was predicted (figure 3B).

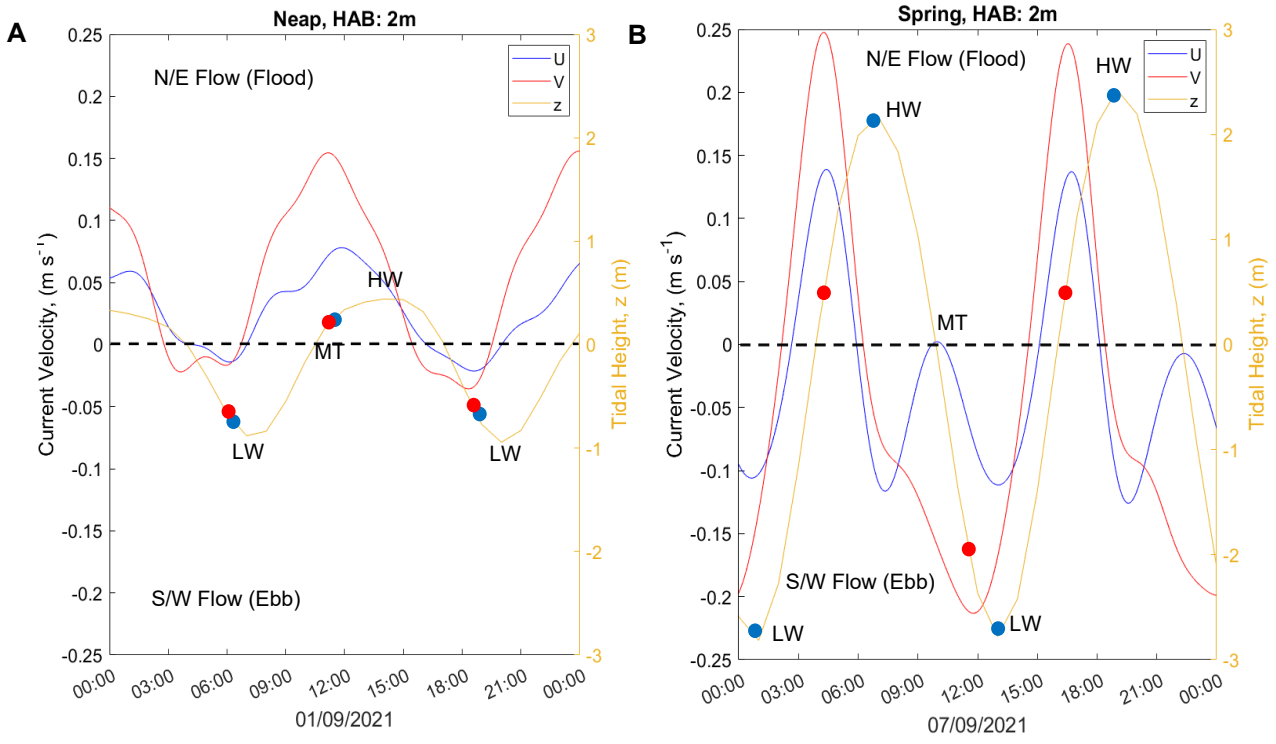

Figure 3: A) U (blue) and V (red) current velocities measured during a 24-hour neap tidal cycle (01/09/21). **B)** U and V current velocities measured during a 24-hour Spring tidal cycle (07/09/21). Both A and B plots are accompanied by the tidal elevation (z) prediction for each period. Black dashed line intercepts both plots at velocity: 0m/s. Positive values are northward and eastward flows; negative values are southward and westward flows. Red and blue dots: positioned on the tidal elevation curve, highlight the tidal stage where maximum V and U current velocities occur respectively.

Inferring local resuspension of SPM from EI

Temporal variations in SPM concentrations were observed vertically throughout the water column during flooding and ebbing tides on the 01/09 (figure 4). Analyses of SPM profiles and EI data were focused between HAB 2-6m. During the flooding tide, averaged SPM concentrations measured ~17% greater at HAB 6m, at mid-tide, relative to values at HAB 2m (figure 4C). This indicated a trend of decreasing SPM concentrations with depth. As the flooding tide progressed towards HW, the reverse was observed; with SPM concentrations ~17% greater at HAB <3m. This data provides evidence that SPM is predominantly in resuspension, throughout the water column, during the mid-tidal flood phase. As the tide progresses towards HW, SPM re-settles, and concentrations increase towards the seabed (figure 4D, E). SPM concentrations ranged from 0.7mg/l to 1.26mg/l throughout the flooding tide, the maximum range of 0.56mg/l was measured at HAB <3m.

In-situ, EI data mirrored the findings of the SPM profile measurements, indicating a relationship between the datasets. A maximum EI value of -6.9dB was measured at HAB 6m, at mid tide, ~4-5dB greater than the maximum values of -10.9dB and -12.2dB measured at 2m and 4m respectively (figure 4B). As the flood progressed, EI decreased at HAB 6m, increasing <4m. A spike in EI was observed at 4m ~11:25am, providing a peak EI value of -6.3dB throughout the flood. As EI then decreased at 4m it increased at 2m, this coincided with a relatively high in-situ SPM value of 1.1mg/l (figure 4).

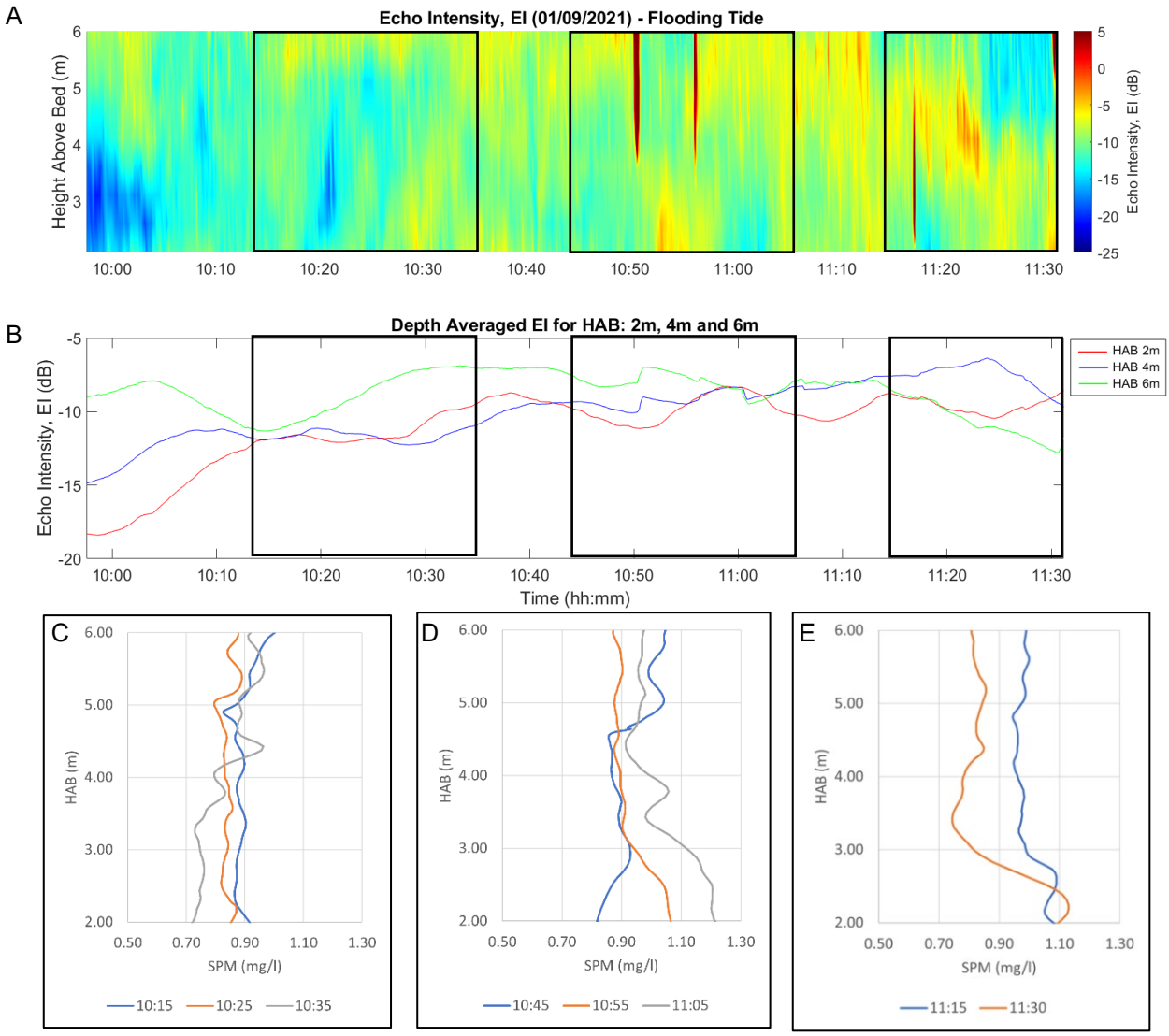

Figure 4: EI and SPM concentrations measured throughout a mid-late flooding tidal phase on the 01/09/2021. **A)** EI timeseries pcolor depicting the temporal variation in EI throughout the flooding tide. **B)** A timeseries of depth averaged EI at HAB: 2,4, and 6m. **C to E)** vertical water column profiles of SPM concentrations. Mid tide: **C**, HW:13:12pm.

EI data provided a detailed time series of temporal variation throughout the water column, measurements identified the complexities of water column property variation, evidencing anomaly EI spikes (figure 4A and B). EI measurements correspond with the 8 in-situ vertical SPM profiles, validating the use of EI data as a proxy measurement of SPM concentration.

The relationship between EI and SPM was further evidenced throughout the ebbing tide. EI was predominantly lower at HAB 6m relative to that observed at 4m and 2m; this was also true for SPM concentrations (figure 5). Multiple peaks of EI were observed throughout the dataset. Firstly, EI reached -5.4dB at HAB 2m, between 14:30pm and 14:50pm (figure 5B). A second peak was observed at 15:25pm, reaching an EI value of -9.5dB at HAB 6m. In-situ SPM data were not captured, therefore inhibiting any direct data comparison at these timings. The maximum SPM value observed throughout the high to mid -tide ebb was

3.62mg/l, almost 3 x the peak SPM value observed during the flood. The maximum SPM value was measured at 15:20pm as EI increased at HAB >4m, indicating that SPM increased in line with EI (figure 5D). The range in SPM concentration was 5 x greater during the ebb relative to the flood, with values ranging from 0.72mg/l to 3.62mg/l. This data suggests that sediment concentrations within the water column are initially relatively homogenous 1hour into the ebb, with small variations in both EI and SPM initially observed (figure 5). SPM profiles evidence the re-suspension process; an initial increase in SPM is observed at depth, values increase into the upper water column as the ebb progresses (figure 5C, D, E).

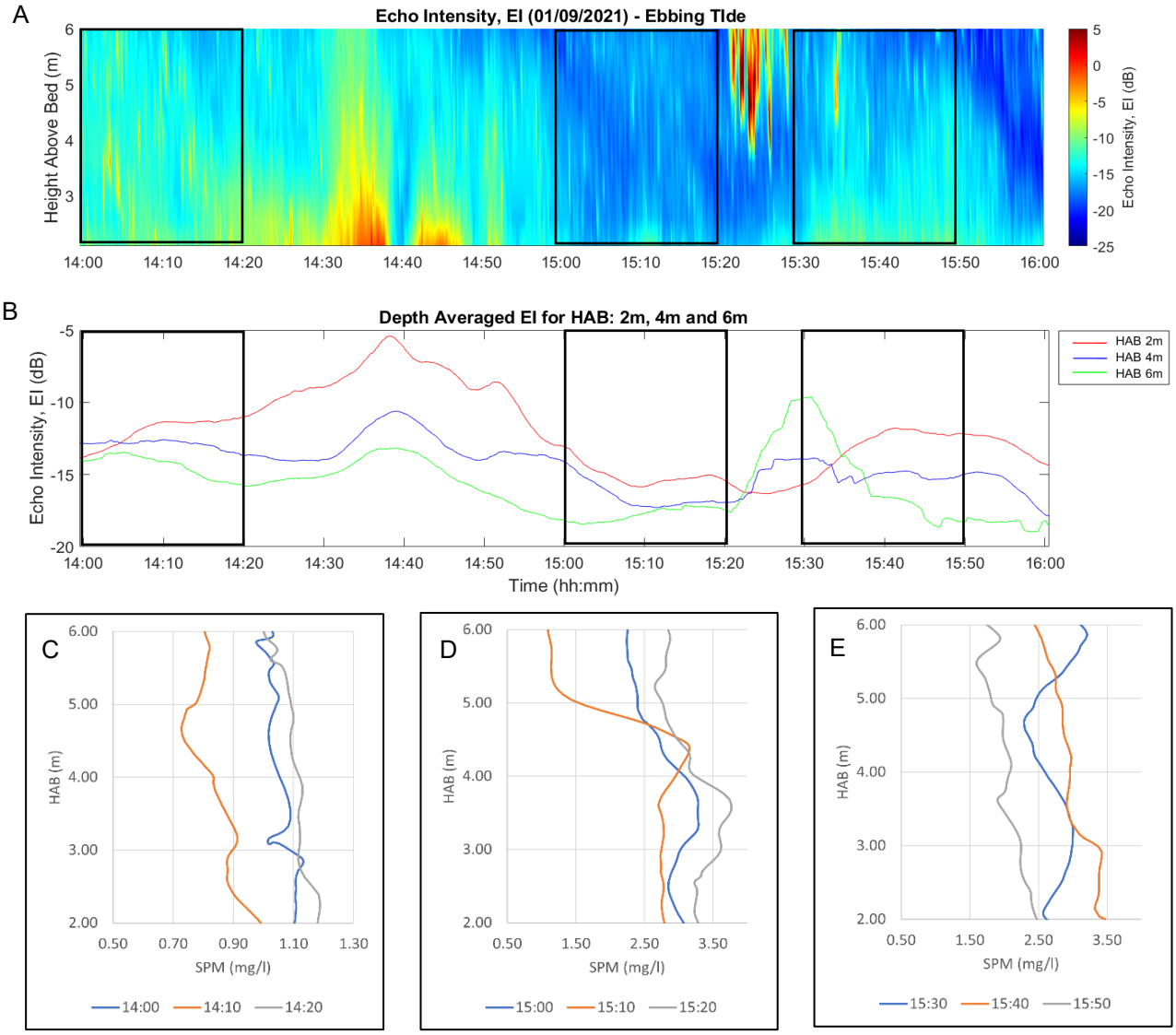

Figure 5: EI and SPM throughout an ebbing tidal phase on the 01/09/2021. All plots incorporate measurements taken between HAB 2-6m. **A)** EI timeseries pcolor depicting the temporal variation in EI throughout the ebbing tide. **B)** A timeseries of depth averaged EI at HAB: 2,4, and 6m. **C to E)** vertical water column profiles of SPM concentrations. LW: 19:49pm.

As with the flooding tide EI dataset, EI data proves water column variation to be more complex, with data showing the lowest EI values occurring between 15:00pm and 15:20pm. However, the greatest EI value was observed at HAB 2m, consistent with the

greater SPM values measured at this time. Upon comparison of SPM profiles together with in-situ EI measurements, it was clear that increases and decreases in SPM values throughout the water column coincided with higher and lower EI measurements respectively.

SPM organic and inorganic fractions

Further analysis of the collected water samples identified that the inorganic fraction of SPM was dominant within all samples (table 4). An average of 76.77% of particulate matter was inorganic and 23.23% was organic. The percentage composition remained consistent throughout all tidal and meteorological conditions, verifying that the SPM throughout the water column was consistently dominated by inorganic matter (table 4).

Table 4: A summary of the inorganic and organic percentages acquired from each stations water sample processing**.**

Date	Station	Time	Tide	% Inorganic	% Organic
07/09/21	S1	10:26	Ebb - Spring	76.25	23.75
07/09/21	S2	10:56	Ebb - Spring	78.57	21.43
29/09/21	S3	14:06	Ebb - Neap	75.49	24.51

A relationship between current velocity, EI, and SPM

Throughout the 7-week data collection period, combined tidal and residual (total) U and V current velocities reached maximum values of 0.28m/s and 0.17m/s in the northward V and westward U direction respectively (figure 6). This extended dataset validates the findings displayed in figure 3, further identifying that the V flow is dominant throughout the dataset and that tidal current velocities are enhanced by residual currents (figure 6). Furthermore, residual currents were consistently observed in the southward V component and the westward U component (figure 6).

There is an evident relationship between EI and current velocity throughout the 7-week dataset (figure 6). A background gradient of EI was observed throughout the timeseries, corresponding to the background tidal current velocity regime. EI consistently increased with increased current velocities; therefore, spring and neap tidal ranges also impacted EI (figure 6). The mean background range in EI, between LW and HW, was ~7dB (neap) and ~16dB (spring). A significant peak in EI was measured on the 27/09 (figure 6). As the tidal phase was transitioning into neap conditions, the EI was expected to decrease in line with the observed regime. However, EI increased from 1.7dB to 29dB throughout the flood, exceeding the mean spring EI range by 58.6%. In-situ total current velocity values measured 0.25m/s in the northward V flow and 0.2m/s in the southward V flow, 25% and 50% greater than the respective tidal velocity flows of 0.2m/s and 0.1m/s. A total westward U current velocity measured 0.13m/s, >4 x the tidal current velocity of 0.03m/s (figure 6); the eastward U velocity was not enhanced.

As this study used EI measurements as a proxy measurement of SPM concentrations, a background gradient in SPM was also identified to be influenced by the tidal regime. In the isolated occurrence of significant EI peaks, it was predicted that SPM concentrations would be significantly amplified. These results identify that the significant increases in current velocities will impact SPM resuspension regimes.

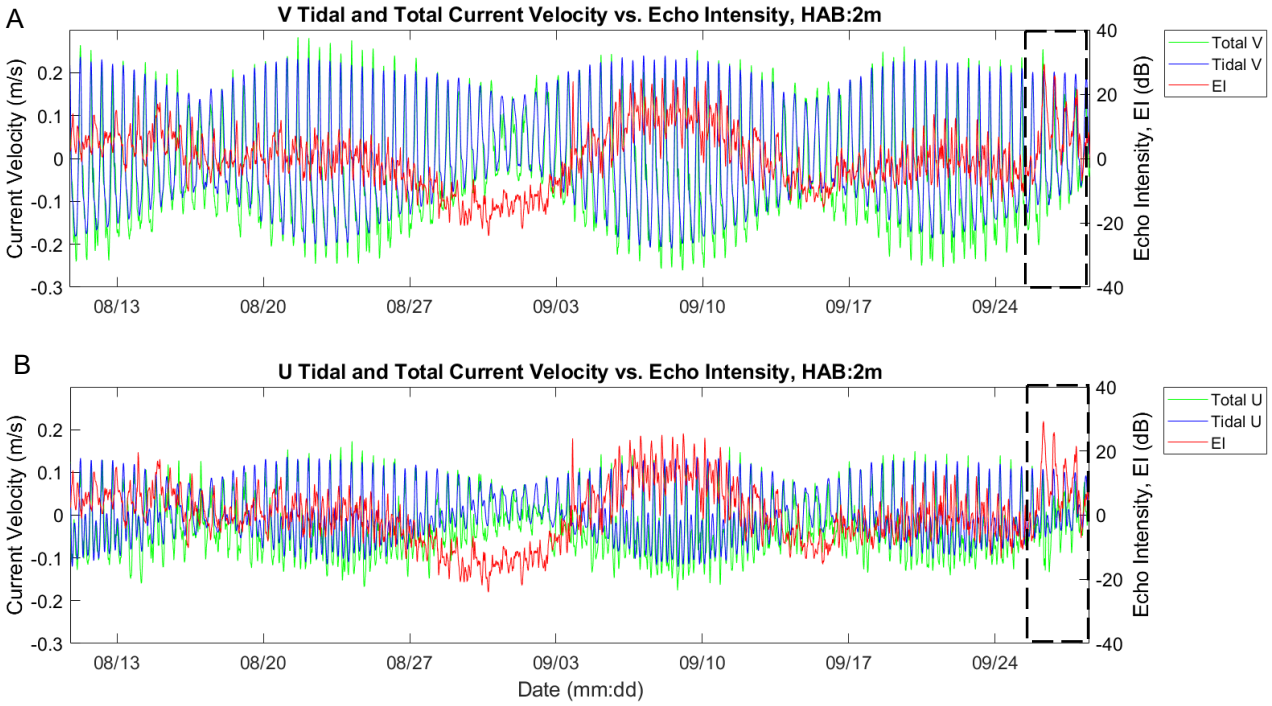

Figure 6: U and V tidal and total (tidal + residual) current velocities throughout the 7-week survey period. Black dashed boxes highlight the anomaly values throughout the dataset relating to the time of a storm surge occurring on the 09/27. **A)** Tidal (blue) and total (green) V velocities; **B)** tidal (blue) and total (green) U velocities. Red: EI measurements taken throughout the survey period. Positive current velocity values: Northward (V), westward (U). Negative current velocity values: southward (V), eastward (U).

The impact of storm events on tidal current velocity regimes

Meteorological and wave data identified that the months of August and September experienced mean wind speeds (WS) of 8.6mph with a mean gust speed (GS) of 12.8mph. The mean H_s was 0.5m with a mean maximum wave height (H_{max}) of 0.7m. A relationship between H_s/H_{max} and WS/WG was identified (figure 7A, B). The mean wave period (T_p) throughout the survey was 6.9s, suggesting that the measured waves were predominantly locally formed wind-driven waves. A significant spike was observed, throughout all variables on the 27/09; H_s measured 2m, with H_{max} reaching the storm wave threshold (determined by PCO) of 3.5m. WS measured 35mph with gusts reaching 55mph.

The maximum WS and H_s measurements obtained on the 27/09 were 4 x greater than the survey period's calculated means. The enhanced forcing of both wind and wave dynamics can be seen to impact the study site within Plymouth Sound; particularly towards the end of the dataset displayed in figure 6. The spikes in EI and current velocities observed in figure 6 coincide with the storm event data displayed in figure 7. This result identifies the influence of external meteorological forcing on the internal hydrodynamics at the study site, particularly on residual currents. Figure 7C demonstrates that the wind direction was consistently northerly throughout September; when wind speeds were enhanced during the identified storm event southward V and westward U current velocities were also enhanced displaying a relationship between wind direction and current flow.

Waves predominantly propagated from the S/SW into Plymouth Sound; constraining enhanced westward current flows.

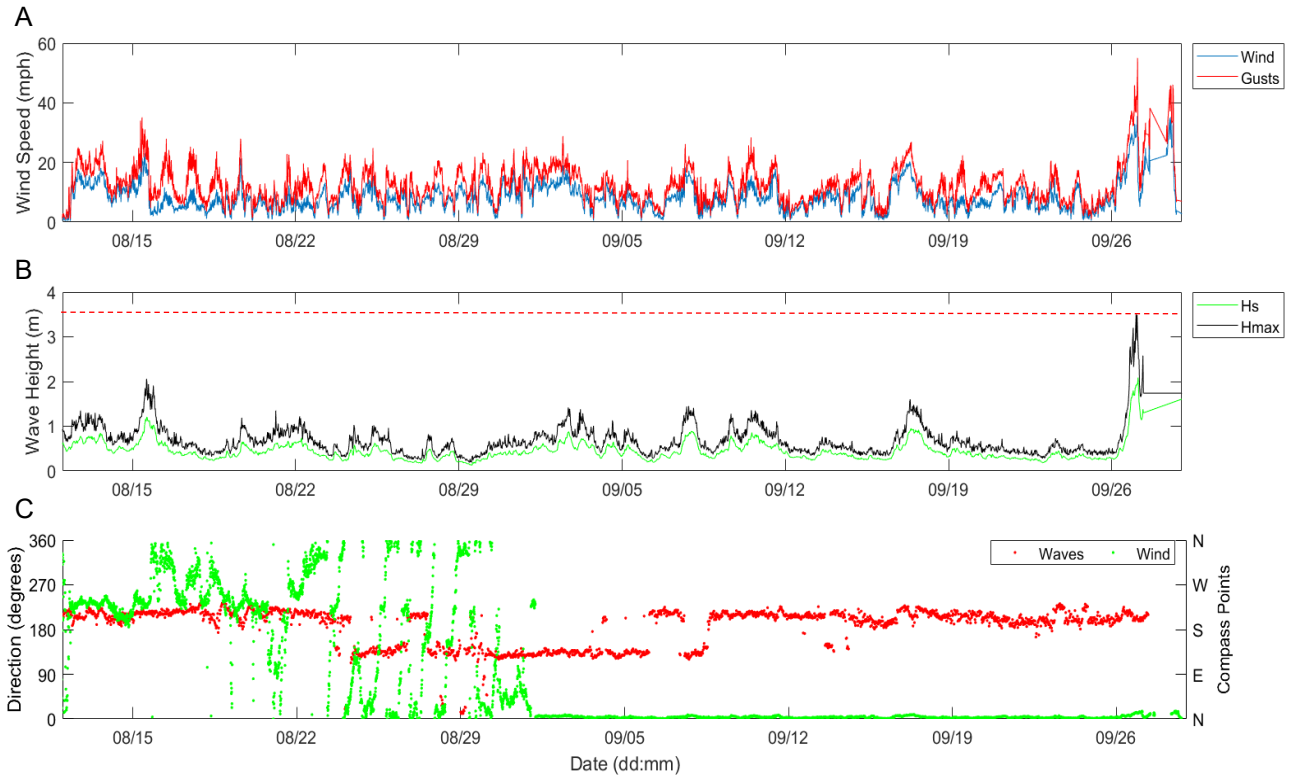

Figure 7: A) Wind speed and gusts. **B)** H_s and H_{max}. **C)** Wind and wave direction throughout the survey period. Red dashed line (B) indicates the storm alert threshold determined by PCO. All data acquired from PCO QC database (PCO, 2022) copyright: Teignbridge DC.

Current velocities' impact on BSS and the resultant influence on SPM

Throughout the neap tidal cycle (01/09), BSS values increased and decreased during the flood and ebb tidal phases respectively, corresponding with the identified increases/decreases in V/U current velocities and EI (figure 8). V current velocities measured on the 01/09, revealed a maximum northward flood current velocity of 0.16m/s, >3 x the maximum southward ebb current velocity, 0.05m/s, and 2 x the maximum measured U velocity, 0.08m/s. These results demonstrated that the flooding V tidal current velocities dominated the tidal movement throughout this neap tidal cycle (figure 8B). The maximum U velocity was also observed during the flood, flowing eastward, resulting in a dominant combined north-eastward flow. This result further confirms a faster flooding tidal phase relative to the ebb, as identified in SPM organic and inorganic fractions. High tide slack water (HTSW) occurred at ~14:20pm, ~1.25 hours after the predicted HW at ~13:12pm (figure 5); at this time, current velocities and BSS measured ~zero, EI measured -11.5dB (figure 8B). Current velocities and BSS values remained low between 14:30pm and 15:00pm as the tide began to ebb; however, EI peaked (See: SPM concentrations and EI), measuring ~2 x the EI at HTSW (figure 8B). It is evident that V tidal current velocities govern BSS throughout both flood and ebb tidal stages (figure 8C).

A maximum BSS value of 0.056N/m^2 was measured at LW +1 hours (01/09), ~20:50pm (figure 8C). During the earlier flood (10:00 – 11:00am) maximum BSS was 0.034N/m^2, measured at LW +3-4hours, coinciding with an increase in EI and peak V current velocities (figure 8). Considering the relationship between BSS, EI, and SPM, this result indicated that sediment resuspension predominantly occurred ~1-4 hours into each flooding tide (figure 8). EI values remained high as BSS decreased, highlighting a time lag between

BSS decrease and SPM re-settlement. Sediment re-settlement was observed during the ebb, corresponding with the maximum EI value, suggesting that SPM concentrations peaked at HAB 2m ~HW +2hours (figure 8B). EI then decreased, suggesting that SPM continued to settle below HAB 2m (beyond this study's datasets). BSS values did not exceed 0.007N/m^2 throughout the ebbing tide, ~12.5% of the maximum BSS flood value; maximum southward V current velocities were also only ~20.5% of the maximum flood V velocities (figure 8C). These measurements indicate a significant reduction in hydrodynamic movement, throughout the mid-low ebb, resulting in reduced SPM concentrations.

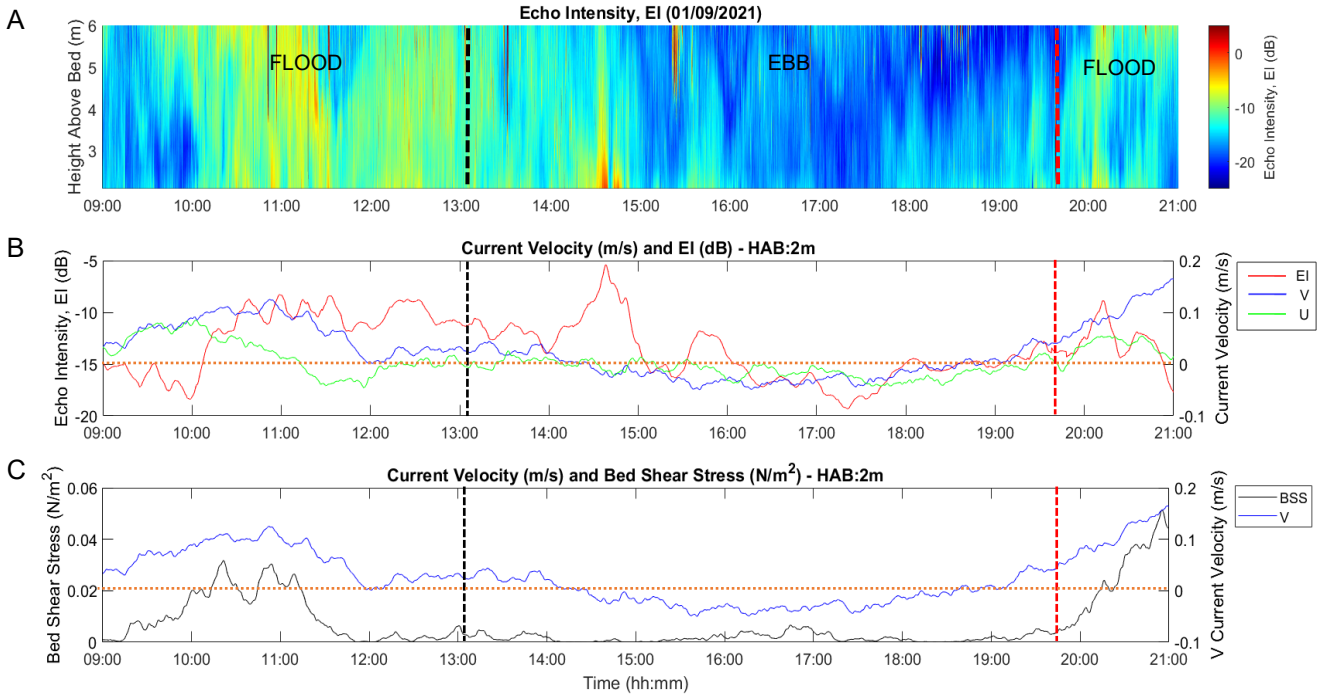

Figure 8: A) EI pcolor plot highlighting the variation in EI throughout the water column HAB <6m. Data is averaged and cleaned and represents 12hours of a 24hour tidal cycle (HW: 13:12pm, LW: 19:49pm). **B)** EI together with the total u and v velocity HAB 2m. Data was smoothed using a 10-minute moving average. Positive current velocity values: northward (V), eastward (U); negative current velocity values: southward (V), westward (U). **C)** Bed shear stress (black) against the total V current velocity (blue) also smoothed using a 10-minute moving average.

A time series of BSS, throughout the 7-week period, was analysed against in-situ current velocity and EI data (figure 9). Results further demonstrated a relationship between all three variables. As previously identified, EI intensified with current velocity; BSS also increased with current velocity, identifying that all three variables were influenced by tidal regimes (figure 9). A spike in BSS occurred on the 27/09 reaching a value of 0.15N/m^2, ~2.6 times the maximum value observed on the 01/09 flood. This uncharacteristic spike in BSS corresponded with the identified spikes of all other variables, suggesting that BSS was also influenced by amplified residual currents.

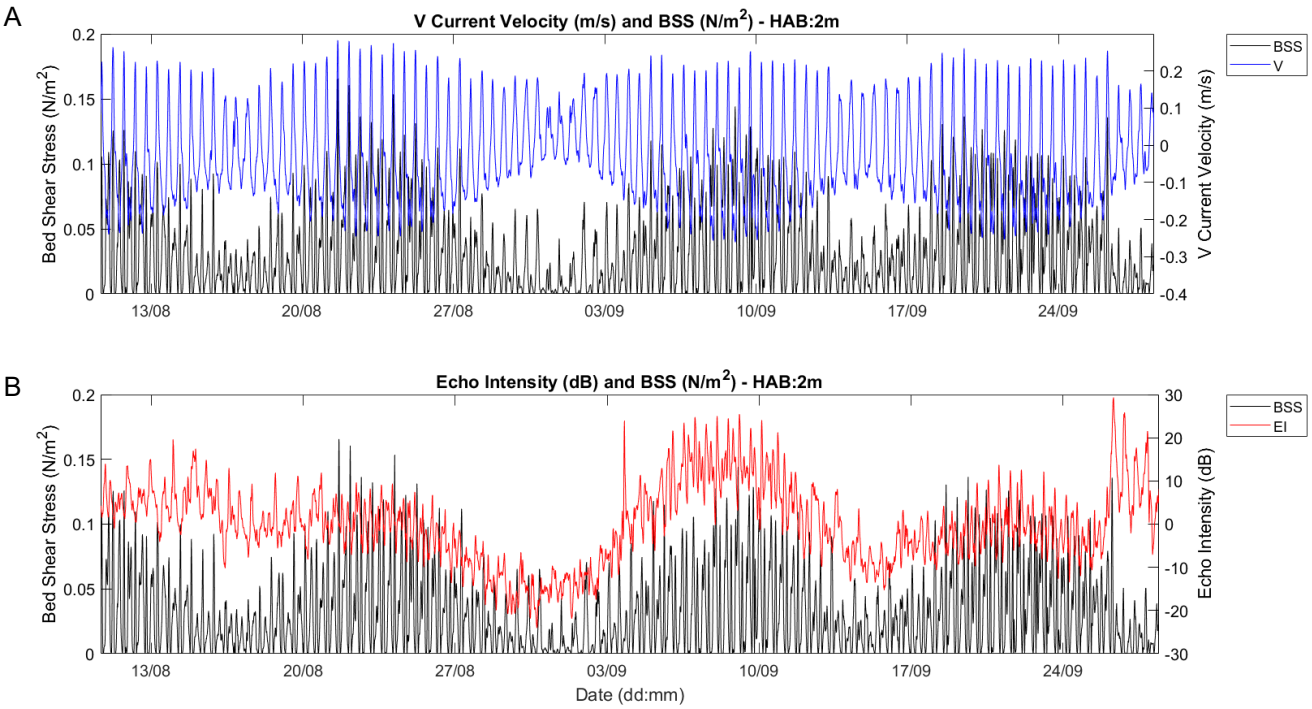

Figure 9: A) BSS (black) and V tidal current velocity (blue) throughout the 7-week timeseries. **B)** BSS (black) and EI (red). All data within this figure has been smoothed with a 1 hour moving average. Positive current velocity values: northward (V), eastward (U); negative current velocity values: southward (V), westward (U).

Discussion

Several reports show seagrass restoration site's SPM concentrations significantly impact restoration success (Ralph *et al*., 2007; Collier *et al.,* 2012; Adams *et al.,* 2016). A strong relationship between SPM concentrations and water quality has been reported in the literature with reduced water clarity impacting seagrass photosynthesis rates (Ralph *et al*., 2007). Moreover, increased levels of sediment re-suspension can also lead to erosion of the plantation site and seedling burial (Cabaço *et al*., 2008), therefore further impacting seagrass restoration success.

SPM concentrations and EI

This study used EI measurements to identify the local SPM resuspension regime within Jennycliff Bay. A clear relationship was observed between SPM and EI values throughout a 12-hour neap tidal cycle; this relationship was also reported by Hill *et al*. (2003) and Chanson *et al*. (2007). Using EI as a proxy measurement for SPM concentration, the current study found SPM measurements throughout the mid-late flooding tide remained relatively consistent between HAB 2-6m. This result suggests SPM is propagated up into the water column as the flooding tide progresses; SPM then remains in suspension throughout the water column during the mid-late flood tidal stage. Peak SPM concentrations were found during the ebb, with maximum values measured ≤ HAB:2m. Maximum ebb SPM values were found to be almost 3 x greater than maximum flood values. The SPM concentration values obtained within this study were in line with those measured previously throughout Plymouth Sound, supporting these studies' findings (Tattersall *et al.*, 2001; Uncles *et al.,* 2015). These results confirm SPM concentrations in the lower water column are significantly increased throughout an ebbing tide, therefore identifying the event of SPM re-settlement. These findings evidence a local SPM

resuspension regime, proving a relationship between tidal regimes and SPM concentrations. This initial finding focused on measurements obtained throughout a 1.1m range neap tide; as identified throughout the 7-week timeseries, it is likely that SPM concentrations will be enhanced during times of increased tidal ranges.

Tidal regimes and SPM resuspension

This study also sought to determine the tidal regime within the study site with the aim to better understand the tidal regimes' influence on SPM concentrations. An important finding demonstrated that the V tidal current velocity dominated the restoration site location. Consequently, this study proceeded to focus on the V tidal current component and was assumed to be the driving tidal factor for variations in SPM concentrations.

When assessing the current velocity measurements throughout the 7-weeks ADCP deployment, a background tidal current velocity regime was identified corresponding to the occurrence of HW and LW. Velocities were found to be greater throughout spring cycle times relative to neaps, confirming that tidal current velocities experienced within the study site were associated with tidal ranges. Interestingly, peak V and U tidal velocities varied in time related to HW and LW. Maximum V and U velocities coincided during neap tidal conditions; however, they varied during springs. This finding identifies relative consistency in the V velocity current component, reaching maximum velocities earlier during the flood, relative to the ebb, throughout both spring and neap tidal cycles.

The identified tidal current regime influenced the measured EI throughout the 7-week period, inferring a clear relationship between tidal current velocities and EI. This finding is consistent with that of previous studies (Hill *et al.*, 2003; Manik *et al.,* 2021). This result supports the earlier observed EI tidal regime and thus SPM, confirming the presence of a local SPM resuspension regime dictated by current velocity and therefore tidal range.

The influence of a storm event on the observed SPM concentrations

A further aim of this research was to determine how increased residual current velocities impacted the background SPM resuspension regime, whilst identifying the cause of amplified residual current velocities. Residual current velocities consistently enhanced tidal current velocities in the southward V and westward U directions throughout the dataset. When comparing meteorological and wave data, there were no external forcing events consistently occurring throughout the dataset. Therefore, the residual currents observed in the south-westward direction were assumed to be caused by other factors.

However, a significant storm event occurred on the 27/09, amplifying wind speeds and H_s. Analysis of these external forces, together with the tidal and total current velocity data, identified that current velocities were predominantly enhanced in the westward direction, with a small enhancement observed in the southward and then northward direction (tide dependent). It was predicted that because the wind increased in the southward direction, V current velocities would also significantly enhance and flow southward; however, this was not the case. This observation was likely due to the opposing S/SW wave direction diminishing the effects of wind forcing. This data confirms a relationship between storm forcing and residual current velocities. It is important to note that these findings also indicate that the impact on current velocities is determined by external forcing direction; it can be assumed that non-opposing wind and wave forcing will significantly amplify the total current velocities observed throughout such a storm event. This result must be interpreted with caution, wind and wave data were acquired outside of the restoration site; therefore, they can only be used as an indication of storm influence on the site's local hydrodynamic regimes.

Enhanced friction at the surface due to external forcing increased current velocities throughout the water column and consequently EI values. According to these data, it can be inferred that SPM concentrations also increased during this storm event, enhancing SPM concentrations beyond the background tidal regime. An implication of this is the probability that during times of enhanced storm events, SPM concentrations will not only increase at depth, but also throughout the water column, resulting in prolonged reductions in water clarity. Consistent with the literature, this finding suggests plantation efforts should be undertaken during settled meteorological conditions, mitigating the potential impact of storm events on the plantation's success. The plantation method could also be adapted to facilitate seasonal instability, allowing for plantation efforts to be more consistent throughout the year.

A relationship between Current velocities, BSS, and SPM

The final important finding was that the north/south (V) tidal current velocity component dictated the amount of friction imposed on the seabed at the study site, consequently determining the BSS. EI values also corresponded to variations in BSS; this result is consistent with those of Carlin *et al*. (2016) who identified that increased BSS resulted in the resuspension of SPM and thus the propagation of sediment upward into the water column. The results obtained from the SPM ashing process confirmed the predominant fraction of the SPM was inorganic; it is therefore likely that sediment suspended from the seabed dominated the SPM composition and influenced BSS. These findings are somewhat limited to the lower water column; however, this was deliberate as seagrasses will be directly affected by hydrodynamics occurring at HAB <2m. However, future research might consider the influence of potential increases of organic matter on upper water column SPM during times of greater biological productivity.

The findings within this study may promote understanding of the optimal timings for seagrass plantation efforts, considering both the background SPM resuspension regime and the impact storm events have on enhancing the assessed variables. A source of uncertainty within this study is the limited measured SPM concentrations used to validate the use of EI as a proxy measurement of SPM; therefore, caution is due when interpreting these results. Several assumptions were used when calculating BSS, for example, sediment grain size, and therefore the bed roughness value. Future studies are recommended to conduct a sediment grain size analysis of the area to better determine the bed roughness, providing a more accurate frictional shear velocity value. Although an assumption was made for bed roughness, this was based on previous research conducted within the area together with the water sample ashing process, confirming the SPM concentrations throughout the water column consisted of predominantly inorganic matter. This result supports the assumption that the particles observed throughout this research predominantly consisted of sediment grains.

Conclusion

This study has identified that greater SPM resuspension occurs throughout flooding tidal phases. Therefore, results indicate that neap mid-late ebb tidal phases are likely to be the most appropriate times to undertake seagrass plantation efforts in Jennycliff Bay. Storm events have been identified to amplify SPM concentrations beyond background values. It can therefore be expected that light penetration will diminish throughout times of enhanced residual currents.

The findings highlight the need for further work. Larger datasets should be used to further validate the use of EI as a proxy for SPM by using water samples obtained throughout a greater range of tidal and meteorological conditions. A grain size analysis of sediment

samples could more accurately quantify the frictional shear velocity throughout tidal cycles, better assessing the impact of BSS throughout the restoration site.

The results evidence the influence of hydrodynamic processes within Jennycliff Bay. Although current velocities are relatively modest within the site, careful consideration must be taken when deciding both plantation methods and timings. For example, the adoption of ASG plantation methods will promote SSL feedback processes enhancing restoration success. This study can not only be used to advise seagrass restoration efforts in Jennycliff Bay, but also highlights the importance of assessing hydrodynamic regimes and local SPM resuspension within any proposed restoration site. Therefore, these findings can be carried forward and used as guidance for future research.

Acknowledgements

Thanks is given to Dr Phil Hosegood, Dr Jill Schwarz and Dr Sarah Bass for the support they have given throughout the development and execution of the research done. Also, to Alex Fraser for his assistance when ashing the sediment samples. Thanks, is also given to the skippers and technicians at the Marine Station for facilitating the fieldwork requirements throughout this research.

Further acknowledgment is given to the Southwest Regional Coastal Monitoring Programme for the use of their quality controlled MetOcean data.

References

Adams, M.P., Hovey, R.K., Hipsey, M.R., Bruce, L.C., Ghisalberti, M., Lowe, R.J., Gruber, R.K., Ruiz-Montoya, L., Maxwell, P.S., Callaghan, D.P., Kendrick, G.A. and O'Brien, K.R. (2016) 'Feedback between sediment and light for seagrass: Where is it important?', *Limnology and Oceanography*, 61(6), pp.1937–1955. Available at: https://doi.org/10.1002/lno.10319 (Accessed: 01 March 2022).

Alekseenko, E. and Roux, B. (2020) 'Risk of wind-driven resuspension and transport of contaminated sediments in a narrow marine channel confluencing a wide lagoon', *Estuarine, Coastal and Shelf Science*, 237, p.106649. Available at: https://doi.org/10.1016/j.ecss.2020.106649 (Accessed: 12 March 2022).

Apostoloumi, C., Malea, P. and Kevrekidis, T. (2021) 'Principles and concepts about seagrasses: Towards a sustainable future for seagrass ecosystems', *Marine Pollution Bulletin*, 173, p.112936. Available at: https://doi.org/10.1016/j.marpolbul.2021.112936 (Accessed: 14 March 2022).

Cabaço, S., Santos, R. and Duarte, C.M. (2008) 'The impact of sediment burial and erosion on seagrasses: A review', *Estuarine, Coastal and Shelf Science*, 79(3), pp.354–366. Available at: https://doi.org/10.1016/j.ecss.2008.04.021 (Accessed: 12 March 2022).

Carlin, J.A., Lee, G-H., Dellapenna, T.M. and Laverty, P. (2016) 'Sediment resuspension by wind, waves, and currents during meteorological frontal passages in a micro-tidal lagoon', *Estuarine, Coastal and Shelf Science*, 172, pp.24-33. Available at: https://doi.org/10.1016/j.ecss.2016.01.029 (Accessed: 01 March 2022).

Carr, J.A., D'Odorico, P., McGlathery, K.J. and Wiberg, P.L. (2012) 'Stability and resilience of seagrass meadows to seasonal and interannual dynamics and environmental stress', *Journal of Geophysical Research: Biogeosciences*, 117(G1).

Carus, J., Arndt, C., Schröder, B., Thom, M., Villanueva, R. and Paul, M. (2021) 'Using Artificial Seagrass for Promoting Positive Feedback Mechanisms in Seagrass Restoration', *Frontiers in Marine Science*, 8, pp.1-7.

Chanson, H., Takeuchi, M. and Trevethan, M. (2007) 'Using turbidity and acoustic backscatter intensity as surrogate measures of suspended sediment concentration in a small subtropical estuary', *Journal of Environmental Management*, 88(4), pp.1406–1416. Available at: https://doi.org/10.1016/j.jenvman.2007.07.009 (Accessed on: 01 March 2022).

Collier, C.J., Waycott, M. and McKenzie, L.J. (2012) 'Light thresholds derived from seagrass loss in the coastal zone of the northern Great Barrier Reef, Australia', *Ecological Indicators*, 23, pp.211-219. Available at: https://doi.org/10.1016/j.ecolind.2012.04.005 (Accessed on: 03 March 2022).

Dyer, K.R. (1997) Estuaries: A Physical Introduction. 2nd edn. Chichester: John Wiley and Sons Ltd.

Fitzpatrick, F. (1991) Studies of sediments in a tidal environment. PhD Thesis. University of Plymouth. Available at: http://hdl.handle.net/10026.1/513 (Accessed: 14 March 2022).

Gacia, E. and Duarte, C.M. (2001) 'Sediment Retention by a Mediterranean Posidonia oceanica Meadow: The Balance between Deposition and Resuspension', *Estuarine, Coastal and Shelf Science*, 52(4), pp.505–514. Available at: https://doi.org/10.1006/ecss.2000.0753 (Accessed: 02 March 2022).

Hemminga, M.A. and Duarte, C.M. (2000) Seagrass Ecology. Cambridge University Press.

Hill, D.C., Jones, S.E. and Prandle, D. (2002) 'Derivation of sediment resuspension rates from acoustic backscatter time-series in tidal waters', *Continental Shelf Research*, 23(1), pp19-40. Available at: https://doi.org/10.1016/S0278-4343(02)00170-X (Accessed: 02 March 2022).

Hyman, A.C., Frazer, T.K., Jacoby, C.A., Frost, J.R. and Kowalewski, M. (2019) 'Long-term persistence of structured habitats: seagrass meadows as enduring hotspots of biodiversity and faunal stability', *Proceedings of the Royal Society B: Biological Sciences*, 286(1912), p.20191861. Available at: https://doi.org/10.1098/rspb.2019.1861 (Accessed: 02 March 2022).

Infantes, E., Orfila, A., Simarro, G., Terrados, J., Luhar, M. and Nepf, H. (2012) 'Effect of a seagrass (Posidonia oceanica) meadow on wave propagation', *Marine Ecology Progress Series*, 456, pp.63–72.

Lawson, S. E., Wiberg, P.L., McGlathery, K.J. and Fugate, D.C. (2007) 'Wind-driven sediment suspension controls light availability in a shallow coastal lagoon', *Estuaries and Coasts*, 30, pp. 102–112.

Lee, K.-S., Park, S.R. and Kim, Y.K. (2007) 'Effects of irradiance, temperature, and nutrients on growth dynamics of seagrasses: A review', *Journal of Experimental Marine Biology and Ecology*, 350(1), pp.144–175.

Luijendijk, A., Hagenaars, G., Ranasinghe, R., Baart, F., Donchyts, G. and Aarninkhof, S. (2018) 'The State of the World's Beaches', *Scientific Reports*, 8(1). Available at: https://www.nature.com/articles/s41598-018-24630-6 (Accessed 16 November 2021).

Manik, H.M. and Firdaus, R. (2021) 'Quantifying Suspended Sediment using Acoustic Doppler Current Profiler in Tidung Island Seawaters', *Science and Technology*, 29(1), pp.363-385. Available at: https://doi.org/10.47836/pjst.29.1.21 (Accessed: 27 February 2022).

Maxwell, P.S., Eklof, J.S., van Katwijk, M.M., O'Brien, K.R., de la Torre-Castro, M., Bostrom, C., Bouma, T.J., Krause-Jensen, D., Unsworth, R.K.F., van Tussenbroek, B.I., and van der Heide, T. (2017) 'The fundamental role of ecological feedback mechanisms for the adaptive management of seagrass ecosystems – a review', *Biological Reviews*, 92, pp.1521-1538.

Orth, R.J., Carruthers, T.J.B., Dennison, W.C., Duarte, C.M., Fourqurean, J.W., Heck, K.L., Hughes, A.R., Kendrick, G.A., Kenworthy, W.J., Olyarnik, S., Short, F.T., Waycott, M. and Williams, S.L. (2006) 'A Global Crisis for Seagrass Ecosystems', *BioScience*, 56(12), pp.987-996.

Paul, M. and Amos, C.L. (2011) 'Spatial and seasonal variation in wave attenuation over Zostera noltii', *Journal of Geophysical Research*, 116(C8).

Pawlowicz, R., Beardsley, B. and Lentz, S. (2002) 'Classical tidal harmonic analysis including error estimates in MATLAB using T_TIDE', *Computers and Geosciences*, 28, pp. 929-937. Available at: https://doi.org/10.1016/S0098-3004(02)00013-4 (Accessed: 02 March 2022).

Plymouth Coastal Observatory (PCO) (2022) 'LoB_waves2021.txt'. Available at: https://coastalmonitoring.org/realtimedata/?chart=98&tab=qc&disp_option= (Accessed: 01 February 2022).

Plymouth Coastal Observatory (PCO) (2022) 'LoB_met2021.txt'. Available at: https://coastalmonitoring.org/realtimedata/?chart=98&tab=qc&disp_option= (Accessed: 01 February 2022).

Ralph, P.J., Durako, M.J., Enríquez, S., Collier, C.J. and Doblin, M.A. (2007) 'Impact of light limitation on seagrasses', *Journal of Experimental Marine Biology and Ecology*, 350(1), pp.176–193. Available at: https://doi.org/10.1016/j.jembe.2007.06.017 (Accessed:02 March 2022).

Reidenbach, M.A. and Thomas, E.L. (2018) 'Influence of the Seagrass, Zostera marina, on Wave Attenuation and Bed Shear Stress Within a Shallow Coastal Bay', *Frontiers in Marine Science*, 5. Available at: https://doi.org/10.3389/fmars.2018.00397 (Accessed: 02 March 2022).

Sofonia, J.J. and Unsworth, R.K.F. (2010) 'Development of water quality thresholds during dredging for the protection of benthic primary producer habitats', *Journal of Environmental Monitoring*, 12, pp. 159-163. Available at: https://doi.org/10.1039/B904986J (Accessed: 01 March 2022).

Soulsby, R. (1997) Dynamics of marine sands. Thomas Telford Publications, London.

Spearman, J., Taylor, J., Crossouard, N., Cooper, A., Turnbull, M., Manning, A., Lee, M. and Murton, B. (2020) 'Measurement and modelling of deep sea sediment plumes and implications for deep sea mining', *Nature Scientific Reports*, 10, 5075, Available at: https://doi.org/10.1038/s41598-020-61837-y (Accessed: 05 March 2022).

Strickland, T.D.H. and Parson, T.R. (1972) A Practical Handbook of Seawater Analysis. Bulletin 167. 2nd edn. Ottawa: The Fisheries Research Board of Canada.

Suykerbuyk, W., Govers, L.L., Bouma, T.J., Giesen, W.B.J.T., de Jong, D.J., van de Voort, R., Giesen, K., Giesen, P.T. and van Katwijk, M.M. (2016) 'Unpredictability in seagrass restoration: analysing the role of positive feedback and environmental stress on Zostera noltii transplants', *Journal of Applied Ecology*, 53(3), pp.774–784.

Tan, Y.M., Dalby, O., Kendrick, G.A., Statton, J., Sinclair, E.A., Fraser, M.W., Macreadie, P.I., Gillies, C.L., Coleman, R.A., Waycott, M., van Dijk, K., Vergés, A., Ross, J.D., Campbell, M.L., Matheson, F.E., Jackson, E.L., Irving, A.D., Govers, L.L., Connolly, R.M. and McLeod, I.M. (2020) 'Seagrass Restoration Is Possible: Insights and Lessons From Australia and New Zealand', *Frontiers in Marine Science*, 7. Available at: https://doi.org/10.3389/fmars.2020.00617 (Accessed 25 March 2022).

Tattersall, G.R., Elliott, A.J. and Lynn, N.M. (2001) 'Suspended sediment concentrations in the Tamar estuary', Estuarine, *Coastal and Shelf Science*, 57, pp.679-688. Available at: https://doi.org/10.1016/S0272-7714(02)00408-0 (Accessed: 17 March 2022).

Uncles, R.J. and Harris, J.A.S. (2015) 'Physical processes in a coupled bay–estuary coastal system: Whitsand Bay and Plymouth Sound', *Progress in Oceanography*, 137B, pp.360-384. Available at: https://doi.org/10.1016/j.pocean.2015.04.019 (Accessed: 17 February 2022).

Unsworth, R.K.F., Collier, C.J., Waycott, M., Mckenzie, L.J. and Cullen-Unsworth, L.C. (2015) 'A framework for the resilience of seagrass ecosystems', Marine Pollution Bulletin, 100(1), pp.34–46.

Unsworth, R.K.F., McKenzie, L.J., Collioe, C.J., Cullen-Unsworth, L.C., Duarte, C.M., Eklof, J.S., Jarvis, J.C., Jones, B.L. and Nordlund, L.M. (2018) 'Global challenges for seagrass conservation', *Ambio*, 48, pp.801-815. Available at: https://doi.org/10.1007/s13280-018-1115-y (Accessed: 25 March 2022).

van der Heide, T., van Nes, E.H., van Katwijk, M.M., Olff, H. and Smolders, A.J.P. (2011) 'Positive Feedbacks in Seagrass Ecosystems – Evidence from Large-Scale Empirical Data', PLoS ONE, 6(1), p.e16504.

van Katwijk, M.M., Thorhaug, A., Marbà, N., Orth, R.J., Duarte, C.M., Kendrick, G.A., Althuizen, I.H.J., Balestri, E., Bernard, G., Cambridge, M.L., Cunha, A., Durance, C., Giesen, W., Han, Q., Hosokawa, S., Kiswara, W., Komatsu, T., Lardicci, C., Lee, K.-S., Meinesz, A., Nakaoka, M., O'Brien, K.R., Paling, E.I., Pickerell, C., Ransijn, A.M.R. and Verduin, J.J. (2016) 'Global analysis of seagrass restoration: the importance of large-scale planting', *Journal of Applied Ecology*, 53(2), pp.567–578. Available at: https://doi.org/10.1111/1365-2664.12562 (Accessed: 02 March 2022).

Walter, R.K., O'Leary, J.K., Vitousek, S., Taherkhani, M., Geraghty, C. and Kitajima, A. (2020) 'Large-scale erosion driven by intertidal eelgrass loss in an estuarine environment', *Estuarine, Coastal and Shelf Science*, 243, p.106910.

Waycott, M., Duarte, C.M., Carruthers, T.J.B., Orth, R.J., Dennison, W.C., Olyarnik, S., Calladine, A., Fourqurean, J.W., Heck, K.L., Hughes, A.R., Kendrick, G.A., Kenworthy, W.J., Short, F.T. and Williams, S.L. (2009) 'Accelerating loss of seagrasses across the globe threatens coastal ecosystems', *Proceedings of the National Academy of Sciences*, 106(30), pp.12377–12381.

Xu, S., Wang, P., Wang, F., Liu, P., Liu, B., Zhang, X., Yue, S., Zhang, Y. and Zhou, Y. (2020) 'In situ Responses of the Eelgrass Zostera marina L. to Water Depth and Light Availability in the Context of Increasing Coastal Water Turbidity: Implications for Conservation and Restoration', *Frontiers in Plant Science*, 11.

Zhou, Y., Liu, P., Liu, B., Liu, X., Zhang, X., Wang, F. and Yang, H. (2014) 'Restoring Eelgrass (Zostera marina L.) Habitats Using a Simple and Effective Transplanting Technique', PLoS ONE, 9(4), p.e92982.